JOURNAL OF AIRCRAFT
Vol. 37, No. 1, January–February 2000

Evaluation of Thin Kevlar–Epoxy Fabric Panels Subjected to Shear Loading

Donald J. Baker*
NASA Langley Research Center, Hampton, Virginia 23681

The results of an analytical and experimental investigation of four-ply Kevlar-49–epoxy panels loaded by in-plane shear are presented. Approximately half of the panels are thin-core sandwich panels, and the other panels are solid-laminate panels. Selected panels were impacted with an aluminum sphere at an energy level of either 2.3 or 5.0 ft ·lb. The strength of panels impacted at 2.3 ft ·lb of energy was not reduced when compared to the strength of the undamaged panels, but the strength of panels impacted at 5.0 ft ·lb of energy was reduced by 27–40%. Results are presented for panels that were cyclically loaded from a load less than the buckling load to a load in the postbuckling load range. The thin-core sandwich panels had a lower fatigue life than the solid panels. The residual strength of the solid and sandwich panels cycled more than 1 million cycles exceeded the baseline undamaged panel strengths. Results of a nonlinear finite element analysis conducted for each panel design are presented.

Introduction

IN lightly loaded fuselage skins, such as helicopters, minimum thickness laminates of four plies usually have more than adequate strength, though the stiffness may be marginal. An economical way to increase the bending stiffness with a minimum weight penalty and manufacturing cost is to use a structural concept that is based on sandwich construction. This class of panels has not been sufficiently evaluated to determine guidelines for their use and their relative merit. Considerable work has been performed on buckling-resistant (thick-core) sandwich panels representative of transport aircraft. A limited amount of unpublished research has been conducted on thin-core sandwich panels, but comparisons have not been made with solid-laminate panels. The scope of the initial program was to evaluate solid and sandwich panels of Kevlar, carbon, and hybrids of Kevlar and carbon subjected to low-energy impact damage and fatigue loading. The panels for fatigue testing were to be cycled from a low load to a load into the postbuckling load range of the panels.

This paper presents the analytical and experimental results of a study of four-ply-thick Kevlar–epoxy panels loaded by in-plane shear. Approximately half of the panels also have a thin middle layer of foam to form a mini-sandwich panel. A finite element analysis for each design configuration was used to determine the initial linear buckling load and geometrically nonlinear responses. The present paper presents results that represent the postbuckling strength and fatigue life of undamaged and damaged solid-laminate and thin-sandwich panels. Fatigue life is determined by cycling the panels through the buckling load and into the postbuckling load range. The results for the thin-sandwich panels are compared with the results for the solid-laminated shear panels.

Panel Design and Fabrication

Two different 8-in.-wide × 13-in.-long panel designs were considered in this investigation. One design is a solid laminate with four plies of ±45-deg, style 285 Kevlar-49 fabric impregnated with 5208 epoxy resin. The total thickness of the solid panel varies from 0.033 to 0.034 in. This panel design is referred to as a solid panel in this paper. The other panel design is a sandwich construction with ±45-deg, style 285 Kevlar-49 fabric plies cocured to a 0.04-in.-thick layer of polymethacrylimide foam (Rohacell WF 51) as the middle layer of the panel. The thickness of the sandwich panel varies from 0.067 to 0.069 in. The foam core is over 90% closed cell and adds approximately 4% to the panel weight. The sandwich test panels are a constant thickness and do not contain a step next to the tabs. The individual test panels were cut from large laminates, and steel load introduction tabs were secondarily bonded to the panel edges to provide the 8-in.-wide × 13-in.-long test area (Fig. 1). The panels were sized such that an existing fixture could be utilized.

Material properties used in the analysis were determined by testing coupons manufactured from the same material batches that were used for the panels. The averages of five replicate tests for each material property are summarized in Table 1.

Test Procedures

All static test panels and selected fatigue test panels had back-to-back rosette strain gauges installed in the center of the panel, as shown in Fig. 1. Out-of-plane displacements for the panels were determined by five linear variable displacement transducers (LVDT) located at the panel center and at quarter points along each centerline. One surface of each panel was painted white to be used with a moiré interferometry technique.

Prior to testing, selected panels were installed in the in-plane shear test fixture[1] and impacted with an aluminum sphere using a low-velocity air gun apparatus. The gun fired a 0.5-in.-diam aluminum sphere with a weight of 0.0065 lb at the panel at two velocities to produce an impact energy of 2.3 or 5.0 ft · lb. The impact energy of 2.3 ft · lb produced damage in the panels, whereas the impact energy of 5.0 ft · lb perforated the panels. The impact site was 3.0 in. from a corner on a diagonal, as shown in Fig. 1. After impact, the panels were inspected to provide a measure of the impact damage. The damaged panels were installed in the test fixture so that the impact damage was located on the tension diagonal for testing.

All tests were performed at room temperature in the as-fabricated condition. No environmental conditioning was performed on any specimen. The 8-in.-wide × 13-in.-long shear panels were installed in an in-plane shear test fixture.[1] The in-plane shear test fixture, test panel, and load introduction frame are shown in Fig. 2, installed in a servohydraulic test machine with a minimum 30,000-lb capacity. Loads were applied to the static test panels at the rate of 600 lb/min (46 lb/in./min), whereas the cyclically loaded panels were cycled at a frequency of 3 Hz to a predetermined maximum load. Maximum loads for the cyclically loaded tests were selected so that failure

Presented as Paper 96-1367 at the AIAA/ASME/ASCE/AHS/ASC 37th Structures, Structural Dynamics, and Materials Conference, Kissimmee, FL, 15–17 April 1996; received 31 January 1999; revision received 13 July 1999; accepted for publication 28 July 1999.

*Aerospace Engineer, Mail Stop 190, Mechanics and Durability Branch, Vehicle Structures Directorate-ARL.

Table 1 Summary of Kevlar-49–5208 epoxy material properties

Property	Value
E_{11}	4.7 Msi
E_{22}	3.34 Msi
G_{12}	0.326 Msi
σ_1	90 ksi
σ_2	62 ksi
τ_{12}	8.5 ksi
ε_{11}	0.017 in./in.
ε_{22}	0.014 in./in.
γ_{12}	0.058
ν	0.18

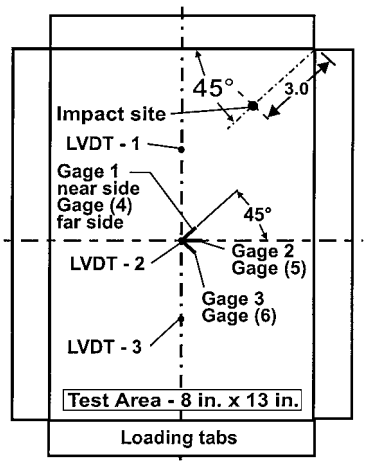

Fig. 1 Location of strain gauges, impact site, and displacement transducers (LVDT).

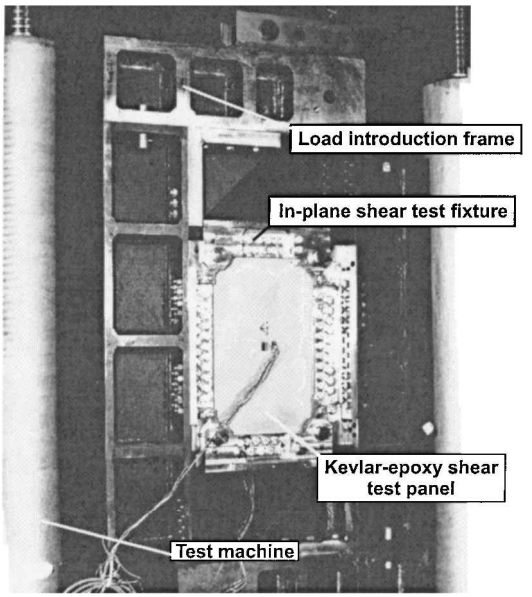

Fig. 2 Test setup with test panel.

would occur at approximately 1 million cycles. The minimum cyclic load was approximately 10% of the maximum cyclic load. Prior to cyclic loading and at selected intervals during the fatigue test, each panel was statically loaded to the maximum cyclic load to determine the in-plane and out-of-plane displacement. Panels that did not fail during cyclic loading were subsequently loaded to failure to determine their residual strength. A still camera recorded changes in the moiré fringe pattern during the static test and static loading to maximum load during the cyclic loading. The load, strain, out-of-plane displacements, and test-machine head displacement were recorded with a computer-controlled data-acquisition system for each test.

Analysis

A finite element analysis was conducted for each design configuration using the STAGS nonlinear structural analysis code[2] to determine the initial buckling load and geometrically nonlinear responses of the panels. STAGS is a finite element code for the general-purpose analysis of shell structures of arbitrary shape and complexity. The STAGS finite element model for the test specimens is shown in Fig. 3. A four-node, quadrilateral shell element, STAGS element 410, was used in the analysis. The test panel contains 416 quadrilateral elements. The finite elements in the test panel have sides of equal length. The test fixture is also included in the model to provide the correct kinematics and boundary conditions for the test panels. The full model has approximately 4200 degrees of freedom. The predicted initial linear buckling load is 16 lb/in. for the solid panels and 158 lb/in. for the sandwich panels. Addition of the thin foam core resulted in an order-of-magnitude increase in the initial buckling load. The same finite element mesh was used for the nonlinear analysis, with the first linear buckling mode shape used as the imperfection with the imperfection magnitude of 10% of the total skin thickness. The Riks method of loading was used in the nonlinear analysis. Selected analysis results are included with experimental results in the following sections.

Results and Discussion

A summary of the results from the static and cyclical load tests of the solid panels and sandwich panels are given in Tables 2 and 3, respectively. The experimental buckling load for each panel is shown in column 4 of Tables 2 and 3. The maximum cyclic load and the number of cycles at the maximum load are shown in columns 5 and 6, respectively. Ultimate panel strength or the residual panel strength after cyclically loading is shown in column 7 of Tables 2 and 3. Figure 4 shows the location of the failures in the panels, where each letter indicates a failure location. Failure locations in each panel are summarized in column 8 of Tables 2 and 3.

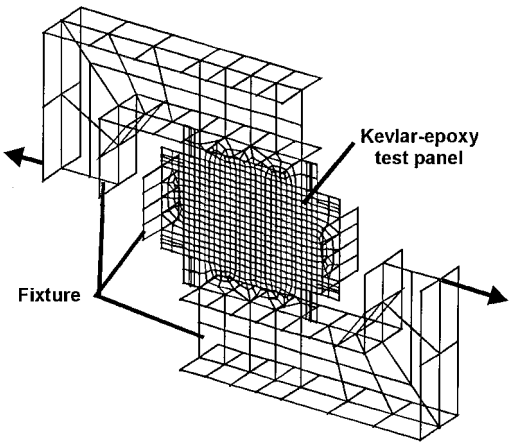

Fig. 3 STAGS finite element model of Kevlar–epoxy panel and loading frame.

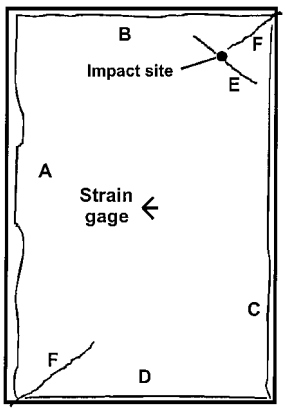

Fig. 4 Location of failure sites.

Table 2 Summary of experimental results for solid panels

Panel no.	Impact velocity, ft/s	Test type[a]	Buckling, lb/in.	Maximum load, lb/in.	Cycles, $\times 10^3$	Strength, lb/in.	Failure locations (see Fig. 4)
SL1	0	S	20	——	——	723	E
SL2	0	S	UD[b]	——	——	545	E
SL3	0	S	UD	——	——	856	A, D
SL4	150	S	UD	——	——	774	E
SL5	153	S	UD	——	——	645	C, E
SL6	224	S	UD	——	——	415	D
SL7	220	S	19	——	——	425	D
SL8	0	F	14	369	385	——	A, B
SL9	150	F	UD	369	102.1	——	F
SL10	150	F	10	369	638.7	——	C, D, F
SL11	220	F	13	270	100	——	B, C
SL12	0	F	DL[c]	576	100	——	A, B, D
SL13	221	F	15	307	1,000	479	D, F, G
SL14	0	F	12	369	1,000	810	B, F, G
SL15	0	F	22	200	3,000	857	A, D, F
SL16	0	F	25	200	10,000	804	A, D, F
SL17	0	F	UD	461	1,005	660	F
SL18	0	F	25	307	5,468	685	——

[a]Test type: S = static and F = cyclic. [b]UD = buckling not defined. [c]DL = data lost.

Table 3 Summary of experimental results for sandwich panels

Panel no.	Impact velocity, ft/s	Test type[a]	Buckling, lb/in.	Maximum load, lb/in.	Cycles, $\times 10^3$	Strength, lb/in.	Failure locations
SW1	0	S	80	——	——	682	B, C
SW2	0	S	80	——	——	657	C
SW3	153	S	DL[b]	——	——	654	A, B
SW4	154	S	DL	——	——	668	F
SW5	258	S	DL	——	——	459	D
SW6	266	S	UD[c]	——	——	518	D
SW7	0	F	75	415	14.1	——	C, F
SW8	0	F	75	415	39.9	——	A, B
SW9	155	F	80	415	23.2	——	E
SW10	151	F	95	415	39.7	——	A
SW11	262	F	57	305	223.9	——	A, B
SW12	264	F	75	305	1000	463	D
SW13	0	F	DL	230	4000	665	C
SW14	0	F	95	160	1000	748	B, C
SW15	0	F	110	192	1000	808	B, F
SW16	0	F	120	184	2000	775	F
SW17	0	F	90	195	DL	——	F, C

[a]Test type: S = static and F = cyclic. [b]DL = data lost. [c]UD = buckling not defined.

Solid Panels

Before testing, selected panels were damaged as noted previously. Damage areas for the solid panels impacted at 2.3 ft · lb of energy are less than 0.06 in.^{2} and are primarily a crazing of the matrix of the plies in the impact area with limited fiber breakage of the far side. There was no measurable dent, and the damage area was very difficult to determine with C-scan methods. The best method to determine the damage area was to view the near side with a bright light shining on the back surface. Damage appeared as a black spot, whereas the rest of the panel appeared yellow. Solid panels impacted at 5 ft · lb of energy were perforated with the 0.5-in.-diam sphere. The edges of the hole were delaminated with the total damage area less than 1.0 in.^{2}

Determination of the initial buckling load of the solid panels is difficult. Only 6 of the 11 undamaged solid panels have a buckling load that can be defined. These buckling loads range from 12 to 25 lb/in., with an average of 20 lb/in. This average buckling load is in good agreement with the predicted buckling of 16 lb/in., considering that the analysis is for perfectly flat panels and that the chance of the test panel in the test fixture being flat is very slim. Every attempt was made to keep the fragile panels flat and supported during installation of tabs, instrumentation, and installation into the test fixture. Even with every effort taken, it would be still possible that the panel as installed in the test fixture would not be flat.

The solid panels generally started deforming out-of-plane with the application of load and continued to form a buckle pattern in the center of the panel that was oriented at 45 deg to the side of the test area. As the load increased, the existing buckles increased in depth, and more buckles started to form at opposite corners and moved toward the center. A moiré fringe pattern indicating the out-of-plane deformation pattern for solid panel SL3 is shown in Fig. 5a. Six half-waves have developed and two more half-waves appear to be starting to form in the corners for an applied load of 850 lb/in. This experimental deformation pattern compares well with the out-of-plane deflections predicted with STAGS nonlinear analysis shown in Fig. 5b for the same applied load. The strain gauge results for panel SL1 are shown in Figs. 6a and 6b. Strain gauges 1 and 4 are parallel to the buckle pattern and indicate a tensile strain from the start of loading up to failure at approximately 0.01 in./in. The dashed line in Fig. 6a is the predicted strain from the STAGS nonlinear analysis. The strains results shown in Fig. 6b are for strain gauges 3 and 6, which are normal to the buckle pattern. The strain gauges initially indicate compression, as expected, and at approximately 20 lb/in. the strain recorded by gauge 3 reverses direction to indicate that the buckling load has been reached. It appears from the load-strain curves that a local failure of the panel may have occurred at 150–180 lb/in. Strains computed in the STAGS nonlinear analysis are also shown in Fig. 6b as a dashed line. The predicted strains

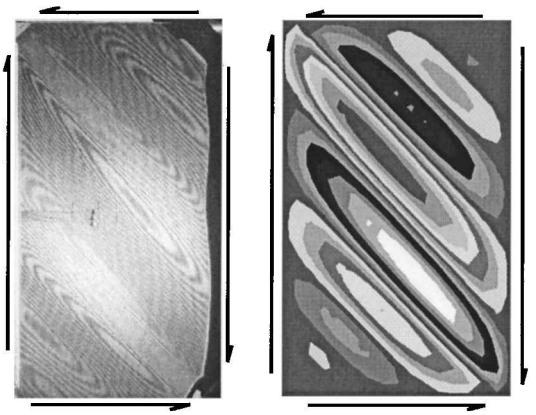

a) Experiment b) Analysis

Fig. 5 Comparison of out-of-plane deflections for solid panel for N_{xy} = 850 lb/in.

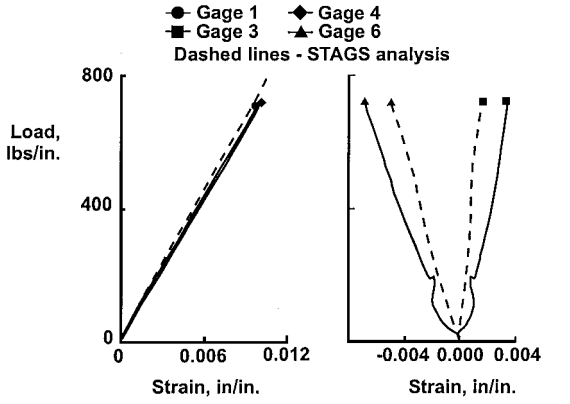

a) Parallel to the buckle b) Normal to the buckle

Fig. 6 Comparison of experimental and predicted strain in panel SL3.

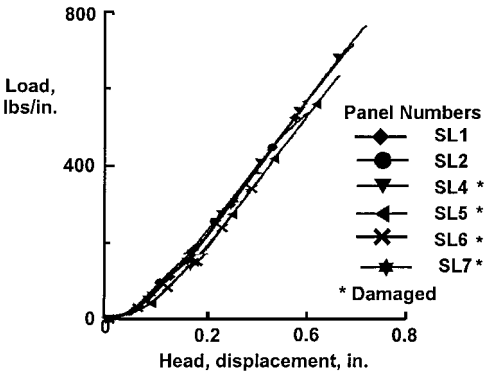

Fig. 7 Comparison of the head displacements for solid panels.

shown in Fig. 6b are at the center of an element and are approximately 0.3 in. from the location of the strain gauge in the test. Good correlation is demonstrated between the experimental strain and the predicted strain. A diagonal tension field, where one diagonal is in tension and the other diagonal is in compression, has developed in these solid panels. These load-strain results are typical of all of the static tests of the solid panels.

Plots of the test-machine head displacement as a function of load are shown in Fig. 7 for six of the static test panels. The test setup was not instrumented properly to be able to compare experimental in-plane displacements with predicted in-plane displacements. Four of the six panels have been damaged, as indicated in Fig. 7. The slopes of these curves are the same for loads greater than 200 lb/in., indicating that the panel in-plane shear stiffnesses are the same. The damage to the panels did not cause a change in the in-plane stiffness. All curves have a small change in slope at 150–180 lb/in., indicating that some change in the response of the panels has occurred.

The average strength (Table 2) of the undamaged solid panels is 708 lb/in. The average strength of the panels impacted at 2.3 ft · lb of energy is 709 lb/in., whereas the average strength of the panels impacted at 5 ft · lb of energy is 59% of the strength of the undamaged panels. The damage from the 5-ft · lb impact causes a significant strength reduction, whereas the damage associated with the 2.3-ft · lb impact does not affect the strength.

A summary of the results for 11 solid panels that were cyclically loaded is shown in Table 2. The maximum cyclic load as a function of load cycles is shown in Fig. 8a. The diamond symbols are considered runout values, and these panels were tested for residual strength, with the results shown in Fig. 8b and Table 2. A curve fitted to the data from the five failed panels is shown as a dashed–dotted line in Fig. 8a. More test results are needed in the low-load, high-cycle region of the plot to complete the fatigue life curve. The average residual strength of the five undamaged solid panels that did not fail after 1–3 million load cycles is 763 lb/in. This average residual strength is 107% of the baseline strength for the undamaged solid panels.

As indicated previously in the Test Procedures section, the cyclically loaded panels were loaded statically at selected intervals to determine whether the static response changes with increased load cycles. The out-of-plane displacement results for panel SL10 are shown in Fig. 9a for initial loading (solid lines) and for a loading after 600×10^3 cycles (dashed lines). It appears as though the material stiffness decreases with increasing number of cycles, thus changing the out-of-plane deflection shape. This decrease in material stiffness did not a have a significant effect on the overall panel in-plane stiffness as shown in Fig. 9b, which plots the head displacement for three load cycles up to 10 million for panel SL16. This phenomenon of decreased out-of-plane deflection with no change of in-plane stiffness was characteristic of all of solid panels that were loaded cyclically. All panels started to crack on the crest of the

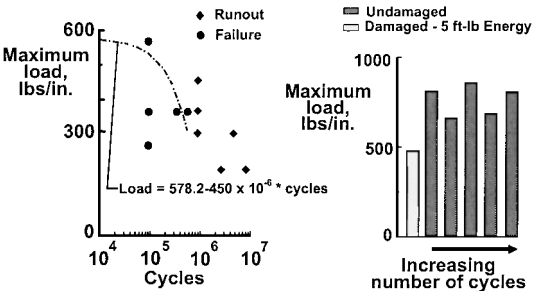

a) Fatigue life b) Residual strength

Fig. 8 Summary of fatigue life and residual strength for solid panels.

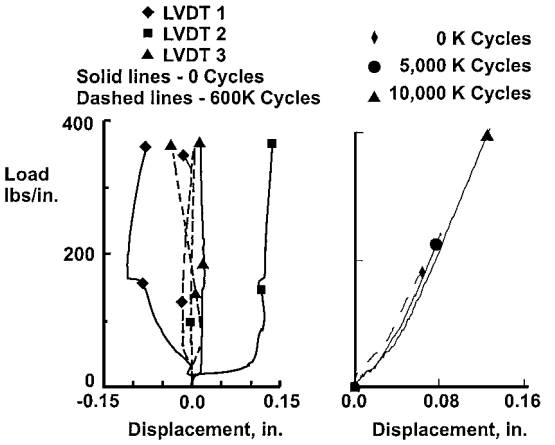

a) Out-of-plane b) In-plane

Fig. 9 Effect of cyclic loading on the in-plane and out-of-plane deflections.

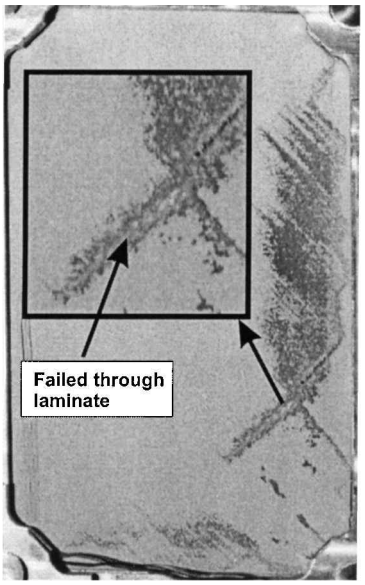

Fig. 10 Photograph of failed panel SL3.

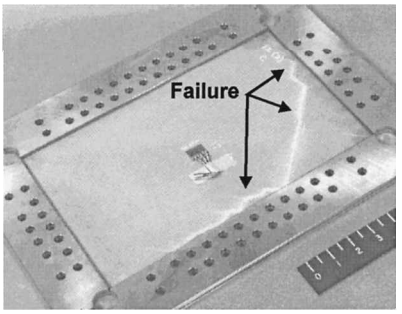

Fig. 11 Failure of damaged panel SL5.

buckle at the panel corners soon after the testing was initiated, and the rate of crack growth varied for the panels. For the damaged panels, the crack propagated to the damage site and stopped for a period before continuing to propagate past the damage site. Crazing of the matrix occurred at various locations adjacent to the steel load introduction tabs. Generally, the solid panels failed by tearing along the load introduction tabs, as shown in Fig. 4. The failure modes for each solid panel are summarized in Table 2 as a combination of letters shown in Fig. 4. Photographs of two failure modes are shown in Figs. 10 and 11. Laminate tension failure occurred in the laminate shown in Fig. 10, which is typical of a diagonal tension failure. Failure of a damaged panel that extends along two sides and through the impact damage site is shown in Fig. 11.

Sandwich Panels

Selected sandwich panels were subjected to low-velocity impact damage at 2.3 or 5.0 ft · lb of energy. The damaged areas for the panels damaged with 2.3 ft · lb of energy are less than 0.25 $in.^2$. The damaged areas for the panels that were perforated (5 ft · lb of energy) with a 0.5-in.-diam sphere are less than 0.6 $in.^2$.

The initial buckling loads are better defined for the sandwich panels than for the solid panels. A summary of the sandwich panel buckling loads is shown in Fig. 12. The average buckling load for the undamaged panels is 91 lb/in., and the average buckling load for the panels damaged with a 2.3-ft · lb impact is 88 lb/in. Panels damaged with a 5.0-ft · lb energy impact buckled at 66 lb/in. or 73% of the undamaged panels. The 91-lb/in. buckling load for the undamaged panels is 58% of the buckling load predicted by the STAGS linear buckling analysis for a flat panel. Although these sandwich panels are thicker than the solid panel, they are still considered fragile and require special handling during manufacture and testing. Even with this special handling, there is no guarantee that the panel was flat when installed in the test fixture. The strain gauge results for panel

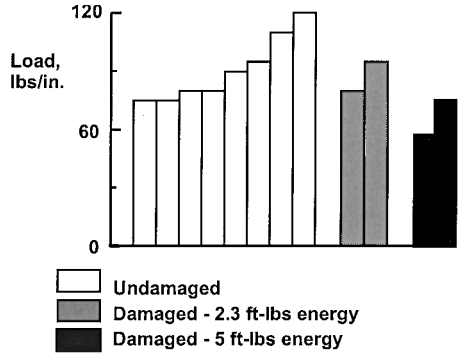

Fig. 12 Summary of initial buckling loads for sandwich panels.

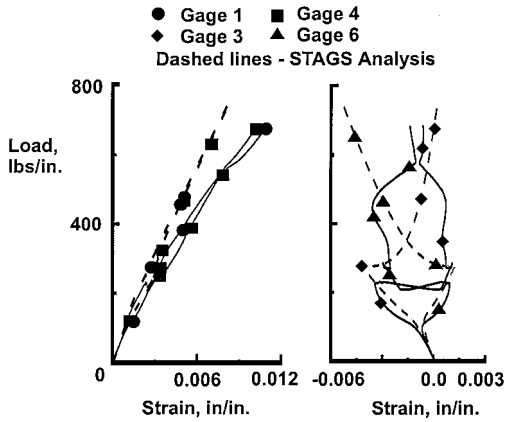

a) Parallel to the buckel b) Normal to the buckel

Fig. 13 Comparison of experimental and predicted strain for panel SW1.

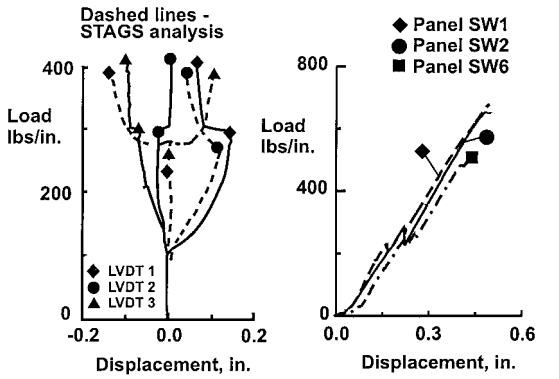

a) Out-of-plane displacements, Panel SW8 b) In-plane displacements

Fig. 14 Comparison of out-of-plane and in-plane displacements for sandwich panels.

SW1 are shown in Figs. 13a and 13b. Gauges 1 and 4 (Fig. 13a) are parallel to the buckle pattern and indicate a tensile strain until failure. The results of the STAGS nonlinear analysis are shown by the dashed lines in Fig. 13a. Strains shown in Fig. 13b are for gauges 3 and 6, which are normal to the buckle pattern. The strains start diverging at approximately 80 lb/in., which is considered to be the buckling load. At 225–240 lb/in. and 550 lb/in., this panel appears to change buckling modes. The STAGS analysis predicted a mode change at 270 lb/in., as shown in Fig. 13b as dashed lines. The predicted strain normal to the buckle pattern has the same trends as the experimental strain. These strain results are typical of all of the static tests of the sandwich panels.

The experimental and predicted out-of-plane deflections for the center (LVDT 2) and the quarter points (LVDT 1 and 3) of sandwich panel number SW8 are shown in Fig. 14a. The experimental results

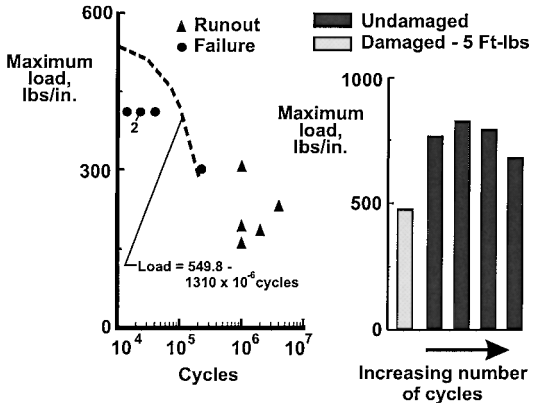

a) Fatigue life b) Residual strength

Fig. 15 Fatigue life and residual strength of sandwich panels.

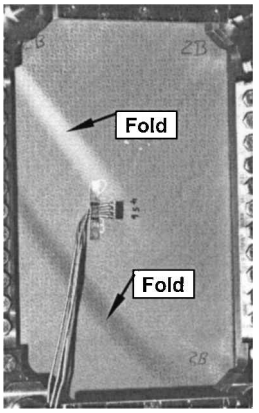

Fig. 16 Photographs of folds in sandwich panel.

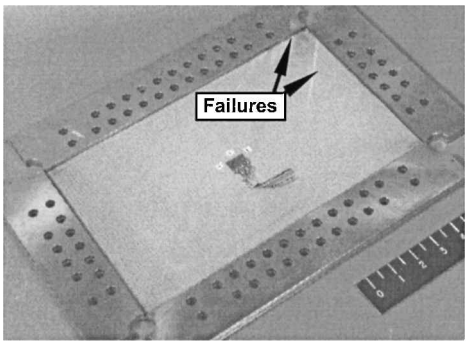

Fig. 17 Failures in sandwich panel.

are from the first static load prior to the start of cyclic loading. A mode change appears to occur at approximately 300 lb/in. for panel SW8. The analysis predicts a mode change at 270 lb/in., as indicated by the dashed curves in Fig. 14a. Good correlation with the analysis is observed up to 70 lb/in. Panel SW8 buckled as two half-waves, as seen by the solid lines in Fig. 14a, where the center LVDT (filled circle) indicated a small deflection and LVDTs at the quarter points indicated larger displacements in opposite directions. The analysis predicted that the panel would buckle as a single half-wave, as can be seen in the dashed lines in Fig. 14a, where the deflection at the quarter points (solid diamond and solid triangle) is small, whereas the deflection at the center (solid circle) is much larger. Plots of the test-machine head displacement are shown in Fig. 14b as a function of load. Panels SW1 and SW2 are undamaged and have nearly the same response, whereas the damaged panel SW6, impacted at 5.0 ft · lb of energy, has larger displacements but its stiffness appears to match the undamaged panels. A load decrease is present in all of the curves and corresponds to the mode change observed in the strain gauge and out-of-plane displacement data, as shown in Figs. 13 and 14a.

The average strength of the panels impacted at 2.3 ft · lb of energy is 661 lb/in., whereas the average strength of the undamaged panels is 670 lb/in. The average strength of the panels impacted at 5.0 ft · lb of energy is 489 lb/in. or 73% of the undamaged panel strength. The strength of the undamaged sandwich panels is 95% of the strength of the undamaged solid panels, whereas the sandwich panels impacted at 2.3 ft · lb are 93% as strong as the solid panels. The sandwich panels impacted at 5.0 ft · lb are 16% stronger than the solid panels.

A summary of the sandwich panels that were cyclically loaded is shown in Table 3, and the maximum loads at failure are shown in Fig. 15a as a function of number of load cycles. A curve fitted to the data from the five failed panels (circle symbols) is shown as a dashed line in Fig. 15a. The triangle symbols represent runout values, and these panels were tested for residual strength, with the results shown in Fig. 15b and Table 3. More test results are needed in the low-load, high-cycle range of the plot to produce a full fatigue life curve for the sandwich panels. The average residual strength of the four undamaged sandwich panels with 1–4 million load cycles is 749 lb/in. This residual strength is 112% of the baseline strength of the undamaged sandwich panels. A comparison of the sandwich panel results in Fig. 15a with the solid panel results in Fig. 8a indicates that the sandwich panels have a shorter fatigue life than the solid panels. The out-of-plane deflections for the sandwich panels also change as the number of cycles increases, as they did for the solid panels. All sandwich panels cracked and failed in a manner similar to the solid panels, and most of the sandwich panels exhibited a fold (Fig. 16), which was set permanently in the panel. A summary of all of the failure modes is given in Table 3 using the notation of Fig. 4. A photograph of a failed sandwich panel is shown in Fig. 17 where one crack extends along the panel edge and another crack extends from the corner parallel to the fiber direction.

Conclusions

The postbuckling strength of thin solid and sandwich Kevlar–epoxy panels has been determined for both undamaged and damaged conditions. Panel fatigue life of the solid and sandwich panels has also been determined for both undamaged and damaged conditions. Low-velocity impact damage caused by a 0.5-in.-diam aluminum ball with 2.3 ft · lb of energy has no effect on the static strength of the solid or sandwich panels, whereas impact with 5.0 ft · lb of energy reduces the panel strength significantly. The static strength of the sandwich panels is approximately 5% lower than the static strength of the solid panels. The fatigue life of the sandwich panels is shorter than the fatigue life of the solid panel. Cyclically loading solid and sandwich panels did not significantly affect the panel residual strength.

References

[1] Farley, G. L., and Baker, D. J., "In-Plane Shear Test of Thin Panels," *Experimental Mechanics*, Vol. 23, No. 1, 1983, pp. 81–88.

[2] Brogan, F. A., Rankin, C. C., and Cabiness, H. D., "STAGS Users Manual," Lockheed Palo Alto Research Lab., Rept. LMSC P032594, Palo Alto, CA, 1994.